CrossMark

ORIGINAL PAPER

First-Principles Study on the Half-Metallic Ferromagnetism and Optical Properties of Fe-Doped CdSe and Co-Doped CdSe

J. H. Tian[1,2] · T. Song[2] · X. W. Sun[2] · T. Wang[2] · G. Jiang[1,3]

Abstract The structural, electronic, magnetic, and optical properties of Fe-doped and Co-doped zinc-blende (ZB) CdSe compounds were calculated and discussed in detail. The Fe-doped CdSe and Co-doped CdSe are found half-metallic ferromagnet with 100 % carrier spin polarization at the Fermi level. The net magnetic moment of $4\mu_B$ and $3\mu_B$ are found per supercell, respectively. The estimated Curie temperature of Fe-doped CdSe and Co-doped CdSe are predicted to be 344 and 210 K, one of which is higher than room temperature. The dielectric functions and the absorption coefficients are studied from the ground electronic states. The impurity states of Fe- and Co-dopants induced strong absorption in the UV-light range and visible region. Overall, Fe-doped CdSe and Co-doped CdSe in the ZB phase show half-metallic ferromagnetic nature and are expected to be potential materials for spintronic devices and optical devices.

Keywords CdSe · Half-metallic ferromagnet · Curie temperature · Optical properties

✉ G. Jiang
gjiang@scu.edu.cn

J. H. Tian
tianjh_lzjtu@163.com

1 Institute of Atomic and Molecular Physics, Sichuan University, Chengdu 610065, China

2 School of Mathematics and Physics, Lanzhou Jiaotong University, Lanzhou 730070, China

3 The Key Laboratory of High Energy Density Physics and Technology, Ministry of Education, Chengdu 610065, China

1 Introduction

In recent years, dilute magnetic semiconductors (DMSs) have been of much interest from the industrial viewpoint, because of their potentiality as a new functional material, which will open a way to introduce the freedom of spin into semiconductor devices [1–3]. For practical applications, it is required to fabricate a high Curie temperature (T_C) ferromagnet with a homogeneous distribution of the magnetic dopants. Doping—the intentional introduction of impurities into a material—is a common approach for tuning the electronic, optical, mechanical, and magnetic properties of materials. Since the original report of ferromagnetism in Mn-doped InAs and GaAs above 100 K [4, 5], II–VI-based semiconductors have been intensively studied for they are a typical semiconductor in which the carrier control technique is well established and they display ferromagnetism when doped with most of the transition-metal (TM) ions, like Mn^{+2} and Fe^{+2}. Partly, substitution of the transition-metal atoms into the cationic site of the host semiconductor results unique physical and magnetic properties [6]. The $3d$ state of transition metal is responsible for the unusual behavior of these materials [7]. Therefore, the investigation of $3d$ state of TM-doped semiconductors is of fundamental physical interest and technological importance [8].

CdSe is a semiconductor with an energy band gap of 1.74 eV at room temperature [9]. It is expected that TM alloys like Fe-doped and Co-doped CdSe can offer half-metallic (HM) ferromagnetic characteristic, so they can be useful in spintronics and other applications. Recently, much effort has been made to improve the properties of CdSe materials by doping Fe or Co. Experimentally, Fe or Co can be doped up to 30 % concentration in the CdSe crystal. Hanif et al. [10] doped $Cd_{1-x}Co_xSe$ at different concentration of Co ($0 \leq x \leq 30$). They confirmed

linear lattice compression with the increasing Co concentration. Orlowski et al. [11] studied the electronic structure of $Cd_{1-x}M_xSe$ (M = Mn, Fe, Co) at 12 and 3 % by ultraviolet photoemission technique. The introduction of transition-metal atoms (Mn, Fe, Co) instead of rare-earth metals in II–VI semiconductors clearly induces magnetic and crystalline disordering in the crystal. Further, they found that the electronic and magnetic properties largely depend on the impurity 3d-electrons and their hybridization with the s-p valence band.

The first-principles pseudo-potential approach has been widely used in material simulations [12–14]. Recent first-principles calculation by Ahmadian et al. [15] indicated that different concentration of V in CdSe could contribute to the magnetic moment in CdSe-based DMSs. However, there is seldom theoretical study on the magnetic and optical properties for Fe-doped and Co-doped CdSe. The aim of this paper is to provide a more accurate and complementary study on the structural, electronic, magnetic, and optical properties of Fe-doped CdSe and Co-doped CdSe with ZB phase using the first-principles technique.

2 Model and Calculation Methods

The lattice constants a of pure ZB phase CdSe is $a = 6.04$ Å. The supercell employed contains 64 atoms which correspond to a $2 \times 2 \times 2$ supercell of CdSe. In the present theoretical studies, two Cd atoms are replaced by Fe/Co in the CdSe crystal to make ordered alloys in the ZB phase. To make our simulation closest to the dilute doping limit, we put the two Fe/Co atoms on positions not adjacent. The doped structures were then optimized with respect to both the lattice constants and the atomic positions.

The optimization of geometrical structures and calculations of the magnetic and electric properties of the ZB compounds were performed using "castep" [16] based on density functional theory. Ultra-soft pseudo-potentials [17] are chosen to represent the interactions between ionic core and valence electrons. The generalized gradient approximation (GGA) and PBEsol [18] are used to describe the exchange and correlation potential. PBEsol is a revised Perdew-Burke-Ernzerhof GGA that improves equilibrium properties of densely packed solids and their surfaces [19, 20]. For the Brillouin-zone sampling, the Monkhorst-pack scheme [21] was adopted. To confirm the convergence of our calculations, we carefully investigate the dependences of the total energy on the cutoff energy from 250 to 850 eV and the k-point set mesh according to the Monkhorst-Pack grid from $3 \times 3 \times 3$ to $12 \times 12 \times 12$, respectively. First-principles electronic structure calculations allow an accurate evaluation of the total energy of a system as a function of the cutoff energy and k-points, and it may be performed with sufficient accuracy to resolve energy differences as small as a few milli electron volts per atom. The test results show that, when the k-point set mesh is fixed in $7 \times 7 \times 7$, the change in total energy is less than 1 meV when the cutoff energy is higher than 550 eV; on the other hand, when the cutoff energy is fixed in 550 eV, the convergence in total energy is very well when the k-point set mesh is beyond $7 \times 7 \times 7$. In consideration of computational accuracy, we choose the cutoff energy to be in 550 eV, and the Brillouin-zone sampling mesh parameters for the k-point set are not lower than $7 \times 7 \times 7$ in this study for CdSe with the ZB structure. The crystal structure and the atomic coordinates are fully relaxed without any restriction using the Broyden-Fletcher-Goldfarb-Shanno method [22] until the force on each atom converges to less than 0.01 eV/Å. The total

Table 1 Calculated lattice constants, bulk modulus and direct band-gap energies of the pure CdSe, Fe-doped CdSe and Co-doped CdSe in the ZB phase

Compounds	Calculations	a (Å)	B (GPa)	Band gaps ($E_g^{\Gamma-\Gamma}$) eV
CdSe	This work	6.077	51.2	1.5
	Exp.	6.077[d]		1.85[d]
	Other Calc.	6.055[a]	54.6[a]	1.73[b]
		6.04[c]	53.2[c]	1.6[c]
		6.217[e]		1.84[e]
$Cd_{1-x}Fe_xSe$	This work	5.93	56.6325	0.4
	Other Calc.	6.03[c]	55.9015[c]	0.5[c]
$Cd_{1-x}Co_xSe$	This work	5.91	56.6381	0.5
	Other Calc.	6.02[c]	55.9084[c]	0.6[c]

[a]Ref. [23]
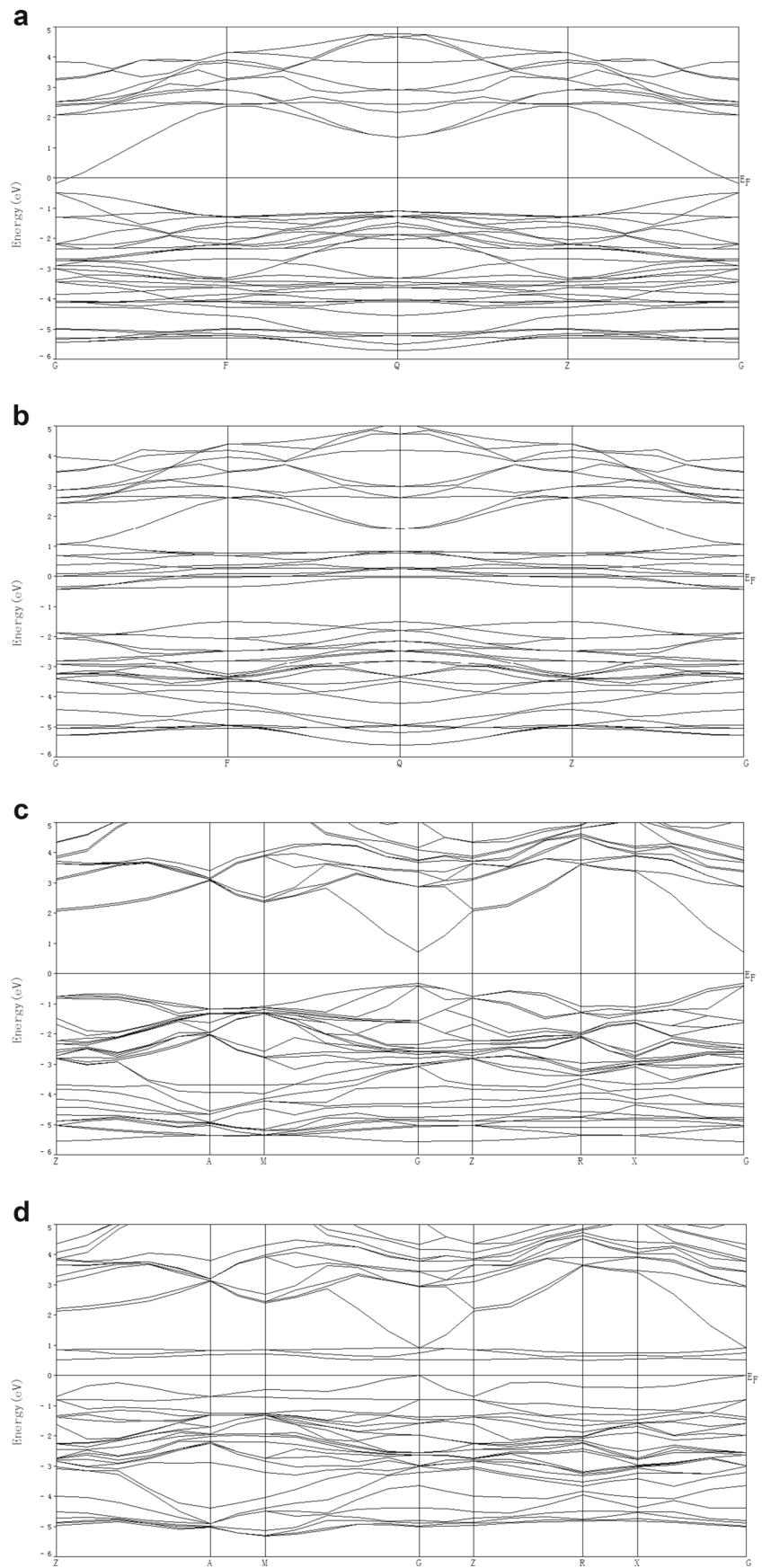[b]Ref. [27]
[c]Ref. [24]
[d]Ref. [25]
[e]Ref. [26]

Fig. 1 The spin-polarized band structure of $Cd_{1-x}Fe_xSe$ for majority spin state (**a**) and minority spin state (**b**), $Cd_{1-x}Co_xSe$ for majority spin state (**c**) and minority spin state (**d**)

energy is converged to lower than 5×10^{-6} eV/atom. The maximum stress of crystal is less than 0.02 GPa. The maximum displacement of atom is less than 5×10^{-4} Å. Then, the electronic band structures and magnetic properties are calculated on the optimized supercells. The valence electron configurations considered in this study included Cd: $4d^{10}5s^2$, Se: $4s^24p^4$, Fe: $3d^64s^2$, and Co: $3d^54s^2$.

3 Results and Discussion

3.1 Structural Properties

The equilibrium lattice constants, bulk modulus, and direct band-gap energies of the pure CdSe, Fe-doped CdSe, and Co-doped CdSe in the ZB phase are calculated and presented in Table 1. The calculated lattices constant for pure CdSe is 6.077 Å, which is in good agreement with the experimental and other simulated results [23–26]. Recently, Arif et al. [24] have reported the optimized lattice constant of 6.04 Å by the full potential linearized augmented plane wave (FPLAPW) method in 2012. The constant of the ZB CdSe 6.055 Å has been reported by Benkabou et al. [23] from the molecular dynamics method. Using the most popular hybrid functional like B3LYP, Xiao et al. [26] calculated the constant of 6.217 Å in 2011. The experimental lattice constant reported by Passler et al. [25] is 6.077 Å. Our result

is in accord with the experimental and other calculated values. This fact will also support the validity of our theoretical predictions of other propertied of CdSe and doped CdSe.

When two Cd atoms in the $2 \times 2 \times 2$ CdSe supercell are replaced by Fe/Co, there are some decrease in the lattice constants to 0.147 Å for Fe doping and 0.167 Å for Co doping after structural optimization, which can be attributed to the fact that the ionic radius of Cd is larger than that of Fe/Co. The results are also in agreement with the experimental results of ref. [10] and the calculated results of ref. [24].

Table 1 also list another structural parameter (bulk modulus) from the GGA + U method for pure CdSe and doped CdSe, respectively. Other theoretical results are also presented for comparison. The theoretical ZB bulk modulus 51.2 GPa is in good accordance with the FPLAPW calculations of Arif et al. [24] and with the molecular dynamics calculations of Benkabou et al. [23]. The calculated bulk modulus of Fe-doped CdSe and Co-doped CdSe are 56.6325 and 56.6381 GPa. The bulk modulus of the material increases with the decrease in the lattice constant.

3.2 Electronic and Magnetic Properties

In order to understand the ferromagnetic properties from the microscopic point of view, we inspect the band structures of both pure CdSe and doped CdSe. The plots of the
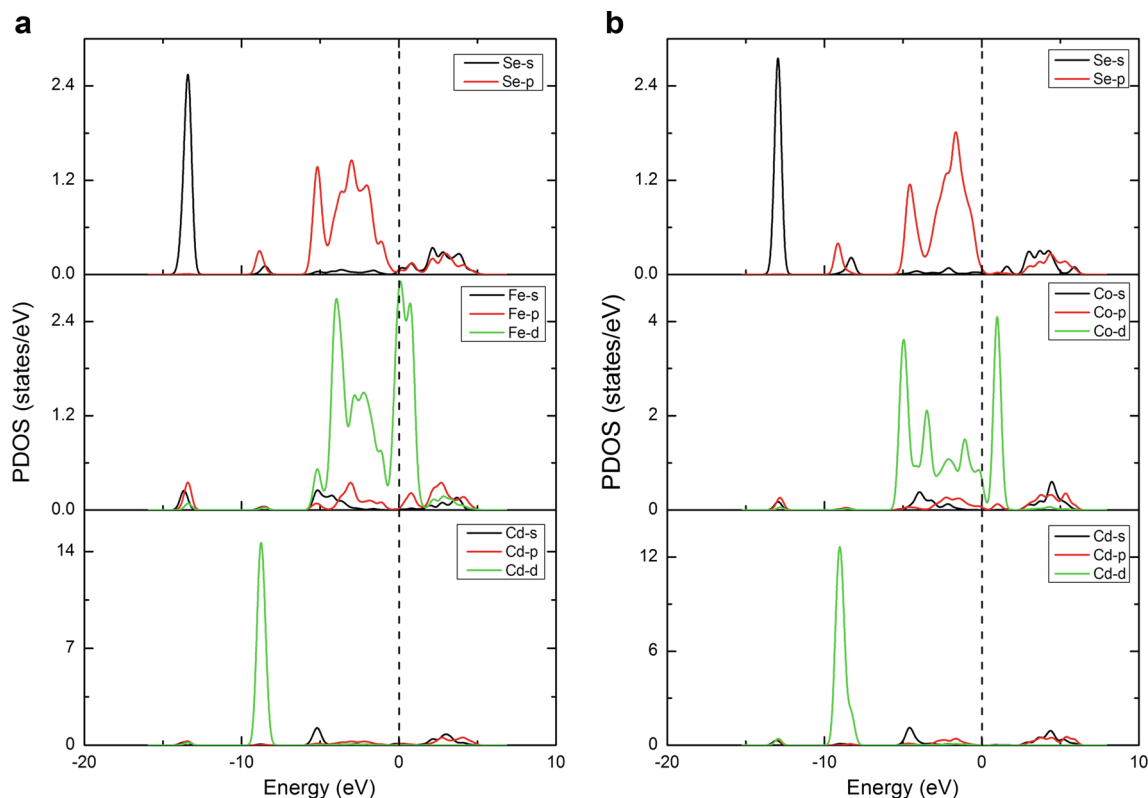

Fig. 2 Partial density of states of $Cd_{1-x}Fe_xSe$ (**a**) and $Cd_{1-x}Co_xSe$ (**b**). Fermi level is set to zero

spin-polarized band structures for Fe-doped CdSe and Co-doped CdSe are presented in Fig. 1. Figure 1a, c is for the majority spin-channels, while Fig. 1b, d is for the minority spin-channels. The top of the valance bands and bottom of the conduction bands are located in the brillouin-zone G symmetry point. After doping, $Cd_{1-x}Fe_xSe$ and $Cd_{1-x}Co_xSe$ ($x = 6.25$ %) are still direct band-gap semiconductors. It shows a half-metallic behavior with the majority spin being semiconductor and the minority spin being metallic with sufficient unfilled states above the Fermi level. These unfilled states behave like free holes, although slightly localized. The 100 % polarization of conduction carriers, which is required in spin injection where highly polarized spin current is desired, suggests that Fe-doped and Co-doped CdSe can be used for spin injection. The calculated band gaps for the pure CdSe and the majority spin-channels are presented in Table 1. Our result is in good agreement with the experimental and other simulated results.

To analyze the detailed electronic structure and the origin of the impurity energy levels of the $Cd_{1-x}Fe_xSe$ and $Cd_{1-x}Co_xSe$ ($x = 6.25$ %), the partial density of states of these systems was calculated, as shown in Fig. 2. It is seen that when Fe- or Co-dopants occupy cation host site Cd, it creates shallow acceptor states, partially fitted, in the top of the valence band. As shown in Fig. 2, the impurity states are mainly dominated by Fe-3d states and Co-3d states, which is in accordance with previous study [24]. From the point of view of the electrical behavior, these impurity states could be considered as the primary origin of the electrical conductivity in the doped CdSe systems.

The total magnetic moment, the atomic magnetic moments, and the magnetization energy were calculated to determine the stable ferromagnetic phase in Fe/Co-doped CdSe systems (see Table 2). The magnetization energy is defined as the difference between the calculated ferromagnetic and anti-ferromagnetic energies ($\Delta E = E_{AFM} - E_{FM}$). A positive value corresponds to stable ferromagnetism. From Table 2, it can be seen that the ferromagnetic state is more stable than the anti-ferromagnetic state, which is also reported in refs. [24] and [28]. It can be clearly seen that $Cd_{1-x}Fe_xSe$ and $Cd_{1-x}Co_xSe$ ($x = 6.25$ %) showed stable ferromagnetic phase with permanent moments of $4\mu_B$ and $3\mu_B$ per supercell, respectively. One can see that the total magnetic moment of $Cd_{1-x}Fe_xSe$ and $Cd_{1-x}Co_xSe$

Table 2 The difference between the ferromagnetic and anti-ferromagnetic energies (meV), total and local magnetic moments μ_B (in Bohr magneton) for $Cd_{1-x}Fe_xSe$ and $Cd_{1-x}Co_xSe$ ($x = 6.25$ %)

Compound	$\Delta E = E_{AFM} - E_{FM}$	M_{tot}	M_{Cd}	$M_{Fe/Co}$	M_{Se}
$Cd_{1-x}Fe_xSe$	2.78	4	−0.02	3.86	0.16
$Cd_{1-x}Co_xSe$	1.69	3	0.04	2.66	0.40

($x = 6.25$ %) mainly originate from Fe/Co atom with small contributions from Cd and Se atoms. It also reveals that Fe-doped CdSe exhibited more stable ferromagnetism than Co-doped CdSe. This is due to the fact that Fe atom has larger magnetic moment than Co atom because of the extra-unpaired electrons in the 3d state of Fe.

The Curie temperature (T_c) can be estimated with the classical Heisenberg model in mean-field theory [18]:

$$k_B T_c = 2\Delta E_{FM}/3x \tag{1}$$

where x is the concentration of doping atoms and k_B is Boltzmann's constant. By (1), the Curie temperature (T_c) of Fe-doped and Co-doped CdSe are obtained. It is about $T_c = 344$ K for $Cd_{1-x}Fe_xSe$ and $T_c = 210$ K for $Cd_{1-x}Co_xSe$ ($x = 6.25$ %) and that of $Cd_{1-x}Fe_xSe$ is higher than room temperature. These results illustrate that Fe-doped and Co-doped CdSe are more promising spintronics materials.

3.3 Optical Properties

The optical properties are studied by dielectric function $\varepsilon = \varepsilon_1 + i\varepsilon_2$; the imaginary part of the dielectric constant (ε_2) can be calculated theoretically based on DFT (see (2)), and then by applying the Kramers-Krönig relation [29], we can evaluate the real part (ε_1) at the same time. The peaks appearing in the ε_2 part of dielectric function are directly related to different intra-band or inter-band transitions in the first irreducible Brillouin zone. The refractive and extinction indices, optical conductivity, and reflectivity were also calculated using (3)–(6) [30–32].

$$\varepsilon_2(w) = \frac{Ve^2}{2\pi\hbar m^2 w^2} \int d^3k \sum_{nn'} |<kn|p|kn'>|^2 f(kn)$$
$$\times (1 - f(kn'))\delta(E_{kn} - E_{kn'} - \hbar w) \tag{2}$$

$$n(w) = \left(\frac{[\varepsilon_1^2(w) + \varepsilon_2^2(w)]^{1/2} + \varepsilon_1(w)}{2}\right)^{1/2} \tag{3}$$

$$k(w) = \left(\frac{[\varepsilon_1^2(w) + \varepsilon_2^2(w)]^{1/2} - \varepsilon_1(w)}{2}\right)^{1/2} \tag{4}$$

$$\sigma(w) = \frac{w}{4\pi}\varepsilon_2(w) \tag{5}$$

$$R(w) = \frac{[n(w) - 1]^2 + k^2(w)}{[n(w) + 1]^2 + k^2(w)} \tag{6}$$

The real and imaginary parts of the dielectric functions were calculated in the range from 0 to 20 eV and plotted in Fig. 3a, b, which demonstrate that the curve shapes of ε_1 and ε_2 are similar for $Cd_{1-x}Fe_xSe$ and $Cd_{1-x}Co_xSe$ ($x = 6.25$ %). The real part of the dielectric function governs the propagation behavior of electromagnetic field in a material. The static dielectric constants $\varepsilon_1(0)$ obtained for
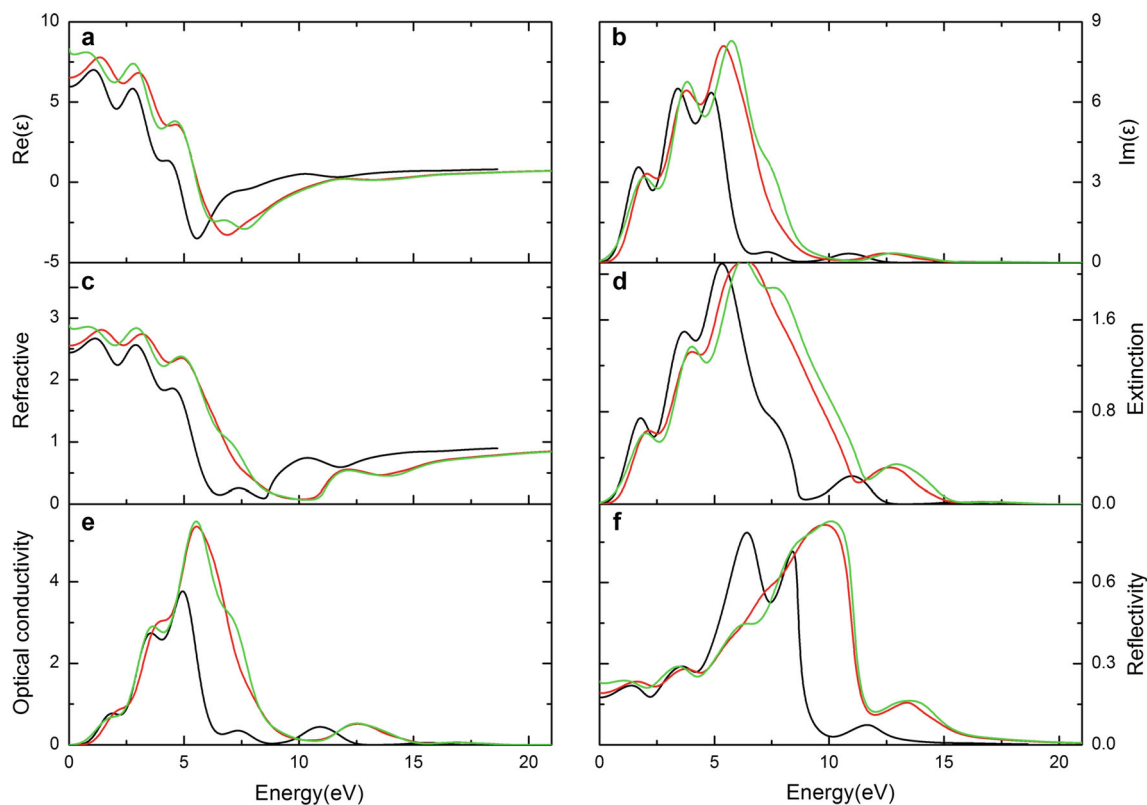
Fig. 3 Real part (**a**) and imaginary part (**b**) of the dielectric function, refractive (**c**) and extinction (**d**) indices, optical conductivity (**e**), and reflectivity (**f**) as functions of photon energy of the pure CdSe (*black line*), $Cd_{1-x}Fe_xSe$ (*red line*) and $Cd_{1-x}Co_xSe$ (*green line*)

CdSe, $Cd_{1-x}Fe_xSe$, and $Cd_{1-x}Co_xSe$ ($x = 6.25$ %) were 5.969, 6.523, and 8.311 respectively, and reach their peaks of 7.006 at 1.06 eV, 7.788 at 1.34 eV, and 8.311 at 0 eV for CdSe, $Cd_{1-x}Fe_xSe$ and $Cd_{1-x}Co_xSe$ ($x = 6.25$ %). The imaginary part of the dielectric function represents the light absorption in the crystal. From Fig. 3b, the onsets of the spectra are at 8.27, 10.15, and 10.50 eV for CdSe, $Cd_{1-x}Fe_xSe$ and $Cd_{1-x}Co_xSe$ ($x = 6.25$ %), respectively. According to Burstein-Moss effect [33, 34], these values are connected with the optical vertical transition from the initial valence band states to the unoccupied states around the Fermi level.

Figure 3c–f shows the refractive and extinction indices, the optical conductivity, and reflectivity of the CdSe, $Cd_{1-x}Fe_xSe$, and $Cd_{1-x}Co_xSe$ ($x = 6.25$ %). From Fig. 3c, the refractive indices in the low region are nearly 2.44, 2.55, and 2.88 for CdSe, $Cd_{1-x}Fe_xSe$, and $Cd_{1-x}Co_xSe$ ($x = 6.25$ %), respectively. In the high region, the refractive indices are all nearly 0.07. The trends of the refractive indices coincide with the real part of the dielectric functions. Figure 3c also shows the intensity of the refractive indices decrease with energy increase, which implies that with the increase of the incident photon energy, the refractive index decreases gradually. As displayed in Fig. 3d, there are three main peaks correspond to that of the imaginary part of the

dielectric functions. The intensity of these three main peaks enhanced and reached the maximum at the third peak. The optical conductivity of CdSe, $Cd_{1-x}Fe_xSe$, and $Cd_{1-x}Co_xSe$ ($x = 6.25$ %) are displayed in Fig. 3e. One can see that when doped with Fe/Co, the peaks of optical conductivity enhanced from 3.76 to 5.35. Figure 3f shows the reflectivity of CdSe, $Cd_{1-x}Fe_xSe$, and $Cd_{1-x}Co_xSe$ ($x = 6.25$ %). It can be seen that the value of the peak did not increase but moved toward high region after doping.

The absorption coefficient $\alpha(\omega)$ can be calculated from the real and imaginary parts of the dielectric function by using the following expressions [35]:

$$\alpha(\omega) = \frac{4\pi}{\lambda} k(\omega) \tag{7}$$

where λ, ω, and $k(\omega)$ represent the wavelength, frequency of the incident light, and extinction indices, respectively. The calculated absorption coefficients of CdSe, $Cd_{1-x}Fe_xSe$, and $Cd_{1-x}Co_xSe$ ($x = 6.25$ %) varying with the wavelength are plotted in Fig. 4. As displayed in Fig. 4, $Cd_{1-x}Fe_xSe$ and $Cd_{1-x}Co_xSe$ ($x = 6.25$ %) have stronger absorption than CdSe, the peaks of absorption coefficients enhanced from 18.2×10^4 to 22.5×10^4 cm^{-1} after doping. $Cd_{1-x}Fe_xSe$ and $Cd_{1-x}Co_xSe$ ($x = 6.25$ %) have similar absorption coefficient curves because of their similar calculated band
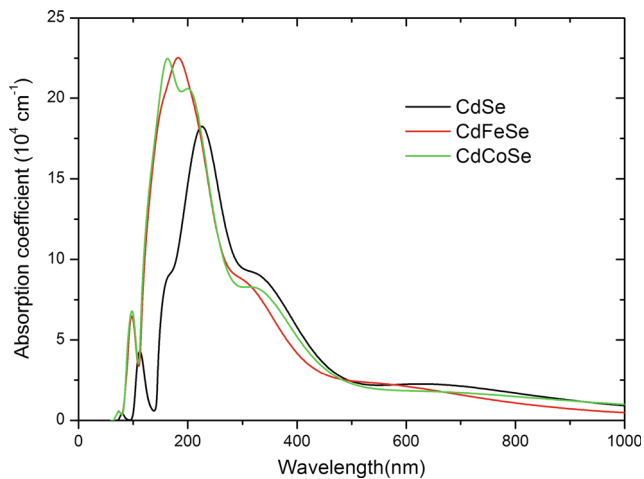
Fig. 4 Calculated absorption coefficients of the pure CdSe, $Cd_{1-x}Fe_xSe$, and $Cd_{1-x}Co_xSe$

element Fe/Co $3d$ with Se $4p$ orbital. The impurity states of Fe- and Co-dopant induced strong absorption in the UV-light range and visible region. In summary, the study of magnetic and optical properties indicates that Fe- and Co-doped CdSe are promising spintronic devices and are potential materials for optical devices, such as absorber of solar cells.

structures. As shown in Fig. 4, the absorption peaks in the wavelength region from 50 to 150 nm and from 150 to 300 nm correspond to the band-to-band transitions. The peaks originate from the transition of the inter-band transitions from the valence band maximum (VBM) to the conduction band minimum (CBM). After doping Fe/Co, the band gap is about 0.4/0.5 eV and is much smaller than 1.5 eV of pure CdSe. As a result, the transition of an electron from valence band to conduction band will need less energy, which may induce intense absorption, improving the photocatalytic property. The inter-band transition was attributed to the Fe/Co $3d$ and Se $4p$ orbital at VBM to the Se $4s$ and Cd $5s$ orbital at CBM. This transition would be more intense compared with that of pure CdSe because of the hybridization between the Fe/Co $3d$ and Se $4p$ orbital at VBM. Figure 4 shows that $Cd_{1-x}Fe_xSe$ and $Cd_{1-x}Co_xSe$ ($x = 6.25$ %) have strong absorption in the UV-light range and visible region. The result indicates that doping with Fe/Co into CdSe is a potential method to make the systems to meet the requirement as the absorber of solar cells.

4 Conclusion

The structural, electronic, magnetic, and optical properties have been studied by GGA and PBEsol. The calculated spin-polarized band structures and magnetic properties reveal that $Cd_{1-x}Fe_xSe$ and $Cd_{1-x}Co_xSe$ ($x = 6.25$ %) are half-metallic ferromagnets. Moreover, the doped systems of $Cd_{1-x}Fe_xSe$ have perfect Curie temperature higher than room temperature. The dielectric functions and absorption coefficients of $Cd_{1-x}Fe_xSe$ and $Cd_{1-x}Co_xSe$ ($x = 6.25$ %) are studied from the electric ground states. The calculated results show that the VBM of the doped systems are attributed primarily to the hybridization of the dopant

References

1. Ohno, H.: Science **281**, 951 (1998)
2. Matsumoto, Y., Murakami, M., Shono, T., Hasegawa, T., Fukumura, T., Kawasaki, M., Ahmet, P., Chikyow, T., Koshihara, S., Koinumaal, H.: Science **291**, 854 (2001)
3. Das, G.P., Pao, B.K., Jena, P.: Phys. Rev. B **69**, 214422 (2004)
4. Munekata, H., Ohno, H., Von Molnar, S., Segmüller, A., Chang, L.L., Esaki, L.: Phys. Rev. Lett. **63**, 1849 (1989)
5. Ohno, H., Shen, A., Matsukura, F., Oiwa, A., Endo, A., Katsumoto, S., Lye, Y.: Appl. Phys. Lett. **69**, 363 (1996)
6. Amin, B., Arif, S., Ahmad, I., Maqbool, M., Ahmad, R., Said, S.G., Prisbrey, K.: J. Electron. Mater. **40**(6) (2011). doi:10.1007/s11664-011-1539-7
7. Arif, S., Ahmad, I., Amin, B.: Int. J. Quant. Chem. (2011). doi:10.1002/qua.23062
8. Ronning, C., Gao, P.X., Dind, Y., Wang, Z.L., Schwen, D.: Appl. Phys. Lett. **84**, 783 (2004)
9. Kittel, C.: Introduction to Solid State Physics, 8th edn. Wiley, New York (2005)
10. Hanif, K.M., Meulenberg, R.W., Strouse, G.F.: J. Am. Soc. **124**, 11495 (2002)
11. Orlowski, B.A., Kowalski, B.J., Chab, V.: Phys. Scr. **41**, 989 (1990)
12. Zakharov, O., Rubio, A., Cohen, M.: Phys. Rev. B **51**, 4926 (1995)
13. Zhang, J.K., Deng, S.H., Jin, H., Liu, Y.L.: Acta Phys. Sin. **56**, 5371 (2007)
14. Zhao, Z.Y., Liu, Q.J., Zhang, J., Zhu, Z.Q.: Acta Phys. Sin. **56**, 6592 (2007)
15. Ahmadian, F., Makaremi, N.: Solid State Commun. **152**, 1660 (2012)
16. Segall, M.D., Lindan, P.J.D., Probert, M.J., Pickard, C.J., Hasnip, P.J., Clark, S.J., Payne, M.C.: J. Phys. Condens. Matter **14**, 2717 (2002)
17. Vanderbilt, D.: Phys. Rev. B **41**, 7892 (1990)
18. Perdew, J.P., Ruzsinszky, A., Csonka, G.I., Vydrow, O.A., Scuseria, G.E., Constantin, L.A., Zhou, X., Burke, K.: Phys. Rev. Lett. **100**, 136406 (2008)
19. Ropo, M., Kokko, K., Vitos, L.: Phys. Rev. B **77**, 195445 (2008)
20. He, L.H., Liu, F., Hautier, G., Oliveira, M.J.T., Marques, M.A.L., Vila, F.D., Rehr, J.J., Rignanese, G.M., Zhou, A.H.: Phys. Rev. B **89**, 064305 (2014)
21. Monkhorst, H.J., Pack, J.D.: Phys. Rev. B **13**, 5188 (1976)
22. Fische, T.H., Almlof, J.: J. Phys. Chem. **96**, 9768 (1992)

23. Benkabou, F., Aourag, H., Certier, M.: Mater. Chem. Phys. **66**, 10 (2000)
24. Arif, S., Amin, B., Ahmad, I., Maqbool, M., Ahmad, R., Haneef, M., Ikram, N.: Curr. Appl. Phys. **12**, 184 (2012)
25. Passler, R.: Phys. Status Solid B **216**, 975 (1999)
26. Xiao, H., Kheli, J.T., Goddard, W.A.: J. Phys. Chem. Lett. **2**, 212 (2011)
27. Streetman, B.G., Banerjee, S.: Solid State Electronic Devices, 5th edn. Prentice Hall, New Jersey (2000). ISBN 0-13-025538-6
28. Amin, B., Ahmas, I.: J. Appl. Phys. **106**, 093710 (2009)
29. Amin, B., Ahmad, I., Maqbool, M., Goumri-Said, S., Ahmad, R.: J. Appl. Phys. **109**, 023109 (2011)
30. Tsafack, T., Piccinini, E., Lee, B.S., Pop, E., Rudan, M.: J. Appl. Phys. **110**, 063716 (2011)
31. Murtaza, G., Ahmad, I.: Physica B **406**, 3222 (2011)
32. Soleimanpour, S., Kanjouri, F.: Physica B **432**, 16 (2014)
33. Burstein, E.: Phys. Rev. **93**, 632 (1954)
34. Moss, T.S.: Proc. Phys. Soc. B **67**, 775 (1954)
35. Harb, M., Masih, D., Takanabe, K.: Phys. Chem. Chem. Phys. **16**, 18198 (2014)